

Spring 2019

Leucine Supplementation in Cuprizone-Induced Oligodendrocyte Toxicity

Michael Ley
mjl110@uakron.edu

Please take a moment to share how this work helps you [through this survey](#). Your feedback will be important as we plan further development of our repository.

Follow this and additional works at: https://ideaexchange.uakron.edu/honors_research_projects

Part of the [Amino Acids, Peptides, and Proteins Commons](#), [Biochemical Phenomena, Metabolism, and Nutrition Commons](#), [Biological Factors Commons](#), [Chemical and Pharmacologic Phenomena Commons](#), and the [Medical Biochemistry Commons](#)

Recommended Citation

Ley, Michael, "Leucine Supplementation in Cuprizone-Induced Oligodendrocyte Toxicity" (2019). *Williams Honors College, Honors Research Projects*. 890.
https://ideaexchange.uakron.edu/honors_research_projects/890

This Honors Research Project is brought to you for free and open access by The Dr. Gary B. and Pamela S. Williams Honors College at IdeaExchange@UAkron, the institutional repository of The University of Akron in Akron, Ohio, USA. It has been accepted for inclusion in Williams Honors College, Honors Research Projects by an authorized administrator of IdeaExchange@UAkron. For more information, please contact mjon@uakron.edu, uapress@uakron.edu.

Leucine Supplementation in Cuprizone-Induced Oligodendrocyte Toxicity

Michael Ley

3150:497

15 April, 2019

Abstract

Cuprizone is a copper chelator that induces demyelination in the central nervous system when fed to mice. This compound is thought to target Complex IV and disrupt mitochondrial metabolism leading to loss of myelin-producing oligodendrocytes. In this proposal, we further examine the chemical and toxicological properties of cuprizone. Immunofluorescence imaging and microarray data on MO3.13 cells treated with cuprizone revealed the possibility of alterations in lysosomal function, as well as mitochondrial disruption via mTOR and Electron Transport Chain (ETC) related pathways. Cell viability assays conducted suggest that addition of Branched-Chain Amino Acids, most commonly used from literature, leucine, can increase cell vitality after being treated with cuprizone. Additional studies examined the solubility of cuprizone and interaction with zinc. Taken altogether, this experiment reveals that cuprizone affects lysosomal and mitochondrial function, and provides insight into leucine supplementation at an attempt to rescue cells from neurotoxicity.

Introduction

Myelin Sheath Function

The myelin sheath plays a vital role in the insulation and conductivity of nerve impulses (**Figure 1**).¹ Myelin is primarily composed of lipids, including membrane-associated phospholipids and cholesterol, and is produced by glial cells known as oligodendrocytes. Oligodendrocytes reside in close proximity with the neuron where they extend and wrap their cell process around an axonal segment. Myelin destruction is seen in autoimmune diseases such as multiple sclerosis (MS), in gene disorders, and after traumatic brain injury.² Demyelination results in the loss or slowing of nerve impulses and axonal degeneration leading to clinical symptoms such as motor and cognitive dysfunction.

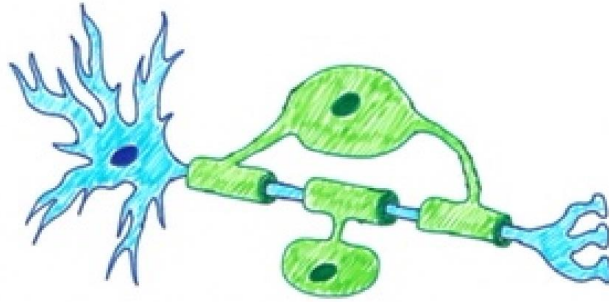


Figure 1. Nerve cell shown in blue insulated by myelin sheath produced by mature oligodendrocytes shown in green.

The Human Oligodendrocytic Cell Line (MO3.13) is used as a model to study oligodendrocyte function *in vitro* (**Figure 2**).³ MO3.13 cells exhibit premature glial cell characteristics and can be induced to differentiate into mature myelin-producing oligodendrocytes or astrocytes.³ These cells are classified as oligodendrocyte precursor cells (OPCs), and exhibit neuronal stem cell properties.⁴

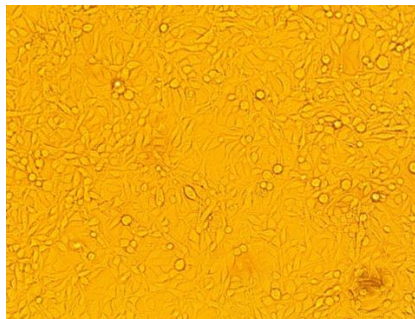


Figure 2. Bright field image of confluent MO3.13 cells at 10x magnification.

The capability of OPCs to differentiate via a stimulus into mature oligodendrocytes poses great possibility for repair of the CNS from both autoimmune and traumatic injury.⁴ The MO3.13 cell line will be used as a model in this experiment to study lysosomal function and leucine supplementation from toxicity in the CNS.

Chelation Properties and Toxicity of CPZ

Cuprizone (CPZ), as seen in **Figure 3**, can act as a copper chelator and has been shown to disrupt mitochondrial function *in vitro* and *in vivo*.⁵ The chelating ability of CPZ has primarily been studied in solution with the absorbance of the Copper-CPZ complex at approximately 600 nm, giving the solution a deep blue color.⁷ However, the chelating abilities of CPZ *in vitro* and *in vivo* have been incompletely defined. Introduction of CPZ has also been linked to altered zinc homeostasis and it is not known if CPZ chelates zinc or other metals along with copper, and if so, if CPZ has a higher affinity for zinc than copper.⁸

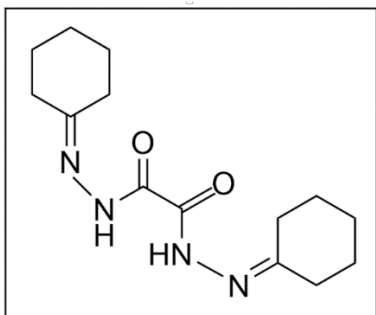


Figure 3. Chemical structure of cuprizone (CPZ) (Chemdraw Professional).

In order to dissolve CPZ into cell media, a solvent such as ethanol (EtOH) along with heating and mixing is needed.¹² Few solubility studies have been done on CPZ in cell media. Two different manufactured CPZ products will be used throughout this experiment to determine whether or not there is a difference between them. These two CPZ powders come from Sigma Aldrich (St. Louis, MO) and Gojira (Bedford Heights, OH) The chelating properties of CPZ to zinc and copper will be tested in this experiment, along with further experimentation on CPZ solubility.

Studies have shown that cuprizone (CPZ) feeding be used as a model in mice to study the processes of demyelination and remyelination as this compound induces loss of myelin in the corpus callosum, hippocampus, and cerebellar peduncles.⁶ The pathology induced by potential copper chelation in the body is complex. One idea is that CPZ binds all available copper, causing a deficiency of copper for oxidative phosphorylation and antioxidant activity.⁹ The terminal electron acceptor in the electron transport chain (ETC) is oxygen, which receives electrons from Cytochrome C Oxidase (COX) and is reduced to water. COX contains two copper binding sites, allowing for the enzyme to participate in redox activity.¹⁰ The redox capability of copper also allows it to help reduce Reactive Oxygen Species (ROS) by accepting electrons.⁹ Through said mechanism of copper chelation, CPZ induces toxicity.¹¹ Oxidative phosphorylation occurs in the mitochondria, along with the localization of many antioxidant enzymes due to the high risk of ROS via the ETC. From this, we predict that the physiology of the mitochondria would be perturbed by the introduction of CPZ.

mTOR Interactions with Branched Chain Amino Acids

The Branched Chain Amino Acids (BCAAs), which include leucine, valine and isoleucine can be broken down for quick energy use by the cell.¹³ The process of degradation of BCAAs starts with a transamination followed by a decarboxylation. After this decarboxylation, each BCAA is broken down by different, but similar, mechanisms. The end products for the breakdown of BCAAs include oxidizable substrates such as acetyl CoA and acetoacetate.¹³ In addition to serving as an energy source, leucine can also activate protein synthesis through signaling by the Mammalian Target of Rapamycin complex (mTOR or mTORC). mTOR is a protein complex that is involved in promoting anabolic reactions. When there are nutrients available in the cell, mTOR signals for synthesis of proteins. When mTOR is active, it

phosphorylates, thus inactivating, the protein ULK1 which promotes autophagy, a process by which cell components are degraded (**Figure 4**).¹⁴

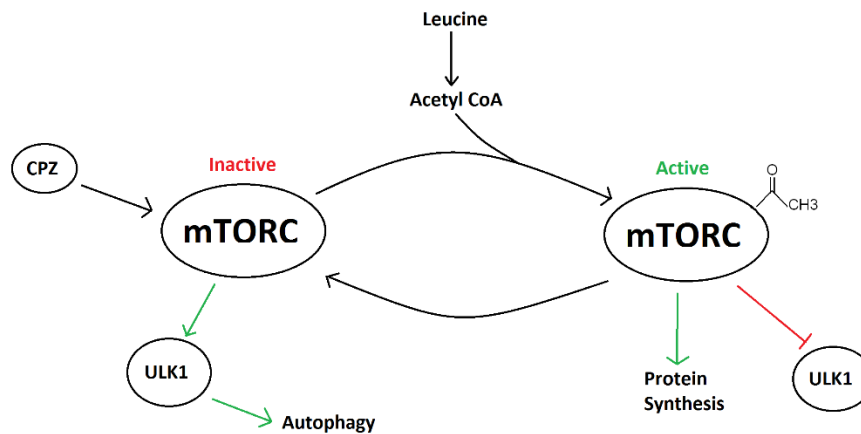


Figure 4. Proposed mTOR complex (mTORC) signal cascade upon addition of CPZ and Leucine.

Swelling in the lysosomes is one of the features that cells undergoing autophagy exhibit.¹⁵ Lysosomes contain degradative enzymes such as proteases that break down the cell during autophagy. Previous experiments have found that excessive ROS generation by CPZ may induce pathological protein misfolding which may lead to the unfolded protein response and the activation of autophagy.¹⁶ This experiment will test three hypotheses: 1) Introduction of CPZ will cause lysosomal swelling, 2) CPZ induces dysfunction in both lysosomal and mitochondrial pathways, and 3) Leucine supplementation will reverse or decrease the toxic effects of CPZ. To test these hypotheses, microarray data of mitochondrial and lysosomal pathways will be analyzed from MO3.13 cells treated with CPZ for 6 hours and 9 hours compared to control untreated MO3.13 cells. Cell viability assays will be conducted to test whether or not leucine supplementation affects CPZ toxicity on MO3.13s. Lastly, fixed cell imaging on MO3.13 cells

treated with CPZ using two lysosome probes, C₁₀ and C₁₁, will reveal lysosomal morphology upon introduction of CPZ.

Materials and Methods

Safety considerations for methods can be found in Appendix 1.

Cell Culture

The MO3.13 human oligodendrocyte precursor cell line from CELLutions Biosystems Inc. (Burlington, Ontario, CA) was kept in a liquid nitrogen dower until needed for culture. To thaw, a 1 mL tube containing a cell line was taken from the dower and kept at room temperature. Once at room temperature, the cell solution and 5 mL of Dulbecco's Modified Eagle Medium (DMEM) with 10% Fetal Bovine Serum (FBS) and 1% Penicillin/Streptomycin (P/S) were added to a T25 flask. The flask was placed in the incubator at 37°C with 5% CO₂. Once the cells grew above 70% confluency in the T25 flask, they were split and plated into T75 flasks. To split the cells, the media was first removed from the flask. The cells were washed with 1X phosphate buffered saline (PBS). After gently shaking the flask, the PBS was removed. To remove the cells from the flask 2 mL of protease, trypsin EDTA, was added and let sit for no more than 3 minutes. The trypsin is then diluted with 3 mL DMEM and transferred to a 15 mL conical tube. The cell solution was centrifuged at 1000 xg at 4°C for 10 minutes. Following centrifugation, the supernatant is aspirated and the pellet is re-suspended into new DMEM with 10% FBS and 1% p/s. This can either be directly aliquoted into cell culture flasks for maintenance of cell line, or counted and aliquoted to various cell experiments.

Cell counts were determined as follows, the newly suspended cell solution from splitting is mixed either by vortexing or inverting. A 20 µl aliquot of cell solution is mixed by titering with 80 µL of Trypan Blue, which stains dead cells blue. The solution is administered into a

hemocytometer which is then placed under a bright field microscope. The hemocytometer contains four grids in which the cells are counted. The average cell count across the 4 grids is used in the calculation to find total cells per milliliter:

$$(\text{Average cell count}) \times (10^4) \times (\text{Dilution factor, 5}) = \text{cells/mL}$$

After the total cells/mL was calculated, $M_1V_1 = M_2V_2$ calculations were conducted to achieve a specific number of cells/well for given experiments.

CPZ Chelation

To test CPZ chelation with copper and zinc, the following solutions were prepared. Stock CPZ solutions for both Sigma Aldrich and Gojira CPZ were prepared at 2 mM in 100% EtOH. The solutions were covered by foil to inhibit rapid evaporation. Stock copper solution was prepared by dissolving copper sulfate, CuSO_4 , into nanopure water at 1 mM. Stock zinc solution was prepared by dissolving zinc perchlorate, $\text{Zn}(\text{ClO}_4)_2$, at 1 mM in nanopure water. After all stock solutions were made, the chelation solutions were prepared: 10 mL of 2 mM CPZ was mixed with 10 mL of 1 mM CuSO_4 and adjusted to pH 8 with 1 M NaOH and absorbance was measured. Afterwards, 1 equivalent of $\text{Zn}(\text{ClO}_4)_2$ was added, absorbance was measured, then 3 equivalents of $\text{Zn}(\text{ClO}_4)_2$ was added and absorbance measured again. The other chelation solution was made by adding 10 mL of 2 mM CPZ with 10 mL of 1 mM $\text{Zn}(\text{ClO}_4)_2$, absorbance was measured, then pH adjusted to 8 and absorbance was measured again. Lastly, 1 equivalent of CuSO_4 was added and absorbance measured.

CPZ Solubility

Stock solutions of CPZ were prepared and diluted to various concentrations depending on the experiment. CPZ powder purchased from Sigma Aldrich (St. Louis, MO) and Gojira

(Bedford Heights, OH) was weighed on a scale, added to ethanol and diluted in dH₂O, PBS or DMEM to reach final volume. The solution was placed in a water bath at 37°C and periodically vortexed until the powder went into solution. The solubility experiments followed the same protocol. Initially, to analyze the solubility of CPZ, many solutions were made varying in concentration, percentage of EtOH, and type of media. The types of media used were DMEM 10% FBS 1% p/s, DMEM 1% p/s (no serum) and Hank's Balanced Salt Solution (HBSS). The concentrations of CPZ were 15 mM, 25 mM and 40 mM. The percentages of EtOH were 20%, 30% and 50%. A total of 27 CPZ solutions were made. The solutions were prepared according to **Table 1**. This represents the solutions made for one type of media, therefore **Table 1** was made in triplicate using each type of media once.

Table 1. Solution recipes for CPZ solubility made in 5 mL of media. Each solution was made once with each media.

	15 mM CPZ	25 mM CPZ	40 mM CPZ
20 % EtOH	20.9 mg CPZ 1 mL EtOH 4 mL Media	34.8 mg CPZ 1 mL EtOH 4 mL Media	55.7 mg CPZ 1 mL EtOH 4 mL Media
30% EtOH	20.9 mg CPZ 1.5 mL EtOH 3.5 mL Media	34.8 mg CPZ 1.5 mL EtOH 3.5 mL Media	55.7 mg CPZ 1.5 mL EtOH 3.5 mL Media
50% EtOH	20.9 mg CPZ 2.5 mL EtOH 2.5 mL Media	34.8 mg CPZ 2.5 mL EtOH 2.5 mL Media	55.7 mg CPZ 2.5 mL EtOH 2.5 mL Media

Once all solutions were prepared, they were placed in the water bath at 37°C with frequent inversions. Images of the solutions were taken after an hour. A second CPZ solubility test was conducted following the results of the MTT assay to try to reduce the percentage of EtOH needed to dissolve the CPZ. This test consisted of 10 mM CPZ 10% EtOH and 10 mM CPZ 5% EtOH. These two solutions were prepared and placed in the water bath with sonication

with frequent vortexing. Images were taken of the solutions after 3 hours. All solutions were prepared in a total of 5 mL of media.

CPZ Microarray

To determine if mitochondrial and lysosomal pathways were perturbed by CPZ toxicity, a microarray study was conducted. Stock CPZ solution was prepared at 1 mM 3% EtOH and was added to MO3.13 cells. After treatment of 6 and 9 hours along with a control group of no treatment, the RNA was isolated with trizol and normalized samples were run in triplicate on the Affymetrix human microarray. The data from the microarray was analyzed to determine pathology of mitochondrial and lysosomal function when introduced to CPZ.

Leucine Supplementation MTT Assay

Living cells will actively reduce yellow colored MTT (3-[4,5-dimethylthiazol-2-yl]-2,5 diphenyl tetrazolium bromide) to formazan crystals due to the presence of NADPH oxidoreductases found in viable cells. This reaction produces a color change from yellow to purple, which can be quantified using a plate reader by taking an absorbance value between 500-600 nm. The amount of MTT reduced, thus the darkness of the purple, correlates with the viability of the cell sample. MO3.13 cells were split and counted to plate 72,000 cells/well in a 96-well plate. The cells were suspended in DMEM 10% FBS 1% p/s and added to each well then placed in the incubator to adhere overnight. Stock CPZ solution was made at 10 mM 30% EtOH and diluted to 1 mM 3% EtOH for treatment. The CPZ solution was added to the 96 well plate following **Table 2** and the plate was placed in the incubator overnight.

Table 2. Treatment on MO3.13s for MTT assay. Each row represents 12 wells (n=12). All solutions were made in DMEM 10% FBS 1% p/s.

	Row
1	1 mM CPZ, 0.8 mM Leucine, 3% EtOH
2	1 mM CPZ, 0.6 mM Leucine, 3% EtOH
3	1 mM CPZ, 0.4 mM Leucine, 3% EtOH
4	1 mM CPZ, 0.2 mM Leucine, 3% EtOH
5	1 mM CPZ, 3% EtOH
6	3% EtOH (Vehicle)
7	No Treatment (Control)

The following day, stock leucine solution was prepared at 5 mM in DMEM 10% FBS 1% p/s then diluted into DMEM 10% FBS 1% p/s to obtain the following treatment concentrations: 0.2 mM, 0.4 mM, 0.6 mM, and 0.8 mM. The leucine solution was added to the 96 well plate following **Table 2**, then the plate was placed in the incubator overnight. The MTT assay was conducted the following day by thawing stock 5 mg/mL MTT solution from the freezer and adding 20 μ L to each well. The plate was then placed in the incubator for 3.5 hours. After incubation the plate was centrifuged at 1000 xg for 10 minutes. The media was removed making sure not to remove any crystals. After the media was removed, 150 μ L of MTT solvent was added to each well, followed by covering the plate in foil. The plate was placed on the orbital shaker for 15 minutes on low speed. Absorbance was read at 590 nm with a reference filter of 620 nm using the Spectramax M2 Plate Reader.

Immunofluorescence

Microscope slide coverslips were cleaned with ethanol and placed one per well into a 6-well plate. A 1 mL aliquot of Poly-L Lysine (PLL) was taken from the freezer and set in the hood to thaw. The PLL was diluted into 9 mL of HPLC grade water and 1 mL was added onto

each coverslip in each respective well making sure to fully cover each coverslip to further increase cell adherence. The 6-well plate was set for at least 1 hour before removing. Once the PLL was removed, the coverslips were washed a few times with HPLC grade water and set to dry in the hood.

For the lysosome imaging, DMEM F-12, 1% p/s was used. This no-serum media was used to ensure that no interactions took place between the FBS, the lysosomal probe and the CPZ. Cells were split and counted as explained. From the results of the cell count, an aliquot of the cell solution was added to DMEM F-12, 1% p/s to reach the final concentration of 10^6 cells/well. This solution was inverted before pipetting 3 mL of cell solution per well into the coated 6-well plate. The 6-well was placed in the incubator overnight to allow for the cells to adhere to the coverslips.

Stock CPZ solutions were individually prepared using both Gojira brand CPZ and Sigma Aldrich (SA) brand CPZ the prior day and were placed in the incubator overnight. The 10 mM stock solutions in 5% EtOH were prepared by weighing 13.9 mg of CPZ and placing it into a 15 mL conical tube along with 250 μ L of EtOH and 450 μ L of DMEM F-12, 1% p/s. The solutions were heated and sonicated with vortexing every 15 minutes. After 3 hours, the CPZ fully dissolved into solution. The vehicle solution was prepared by adding 250 μ L of EtOH into 450 μ L of DMEM F-12, 1% p/s and inverting. The stock CPZ solutions and vehicle were diluted to 2 mM 1% EtOH for treatment. The cells were treated according to **Table 3**. Both the C₁₀ and C₁₁ probes generously provided by Dr. Yi Pang's laboratory were tested using Sigma Aldrich CPZ. The C₁₁ probe was also tested using Gojira CPZ. After treatment, the plate was placed in the incubator overnight.

Table 3. Treatment of MO3.13 for lysosomal imaging.

No Treatment (Control)	2 mM SA 1% EtOH	1% EtOH (Vehicle)
2 mM Gojira 1% EtOH	2 mM SA 1% EtOH	1% EtOH (Vehicle)

After treatment, the coverslips were fixed for cell imaging. For fixing cells, 4% paraformaldehyde (PFA) was prepared. PFA was made in the hood by weighing 1 g of PFA powder (Sigma Aldrich) and adding it to 15 mL of 1X PBS. This solution was heated to 60°C while stirring until the powder was dissolved. The pH was adjusted to 7.4 with additions of 1 M NaOH. 10 mL PBS was then added to reach the final volume of 25 mL and the solution was filtered through a 45 µm syringe filter and stored in a 50 mL conical tube until use. Once PFA was prepared, the treated 6-well plate was aspirated to remove the cell media and 2 mL of PFA was added to fix the cells for 10 minutes. The PFA was then removed and the cells were washed twice with 1 mL of PBS per well. The following steps occurred with all lights off; The C₁₀ and C₁₁ lysosome probes were weighed and added to 1 mL each of DMSO to attain a 10 mM solution (5.72 mg of C₁₀ and 5.42 mg of C₁₁). To dilute to treating concentration of 1 µM, 1.5 µL of each probe was added to 15 mL of PBS. The solutions were inverted to mix and then 1 mL was added to each well. After 30 minutes the solution was aspirated off and the cells were washed 2 times with PBS. To stain the nuclei, DAPI solution was made by diluting a 1 mL aliquot of stock DAPI in 10 mL of PBS which was then added in 1 mL aliquots to cover each well for 5 minutes. The DAPI solution was then removed and the cells were washed with PBS 2 times before washing with HPLC grade water for 10 minutes. The coverslips were left to sit in the water under the

hood until mounting. To mount the coverslips onto microscope slides, a drop of flouromount aqueous mounting medium was applied to the microscope slide. The coverslips were removed from the wells using sterile tweezers and were placed face down onto the slides where the mounting medium was applied. The coverslips were gently laid onto the slides to prohibit bubbles from forming and to create a proper seal. Once placed onto the slides the coverslips were not moved so that the cells stayed intact. After all coverslips were mounted to the slides, the slides were covered in foil and left in the refrigerator to dry for 24 hours. Once dry, clear nail polish was applied around the edges of the coverslips to complete the sealing process. Once sealed the slides were wrapped in foil and stored in the refrigerator until imaging.

Fixed microscope slides were imaged with Nikon A1 Plus Confocal Microscope in Dr. Konopka's lab at both 60x and 100x magnification. The excitation lasers were set to 405 nm for C₁₀ and C₁₁ lysosome probes, and DAPI. The emission filter was set from 640 nm to 715 nm for the lysosome probes and 425 nm to 475 nm for DAPI.

Results and Discussion

Cuprizone Chelation and Solubility:

Both Gojira CPZ and SA CPZ were added to copper and zinc to determine the chelating properties of CPZ. There were no significant differences in chelation between the Gojira CPZ vs the SA CPZ. Unbound CPZ absorbs around 250 nm (**Figures 5-7**).

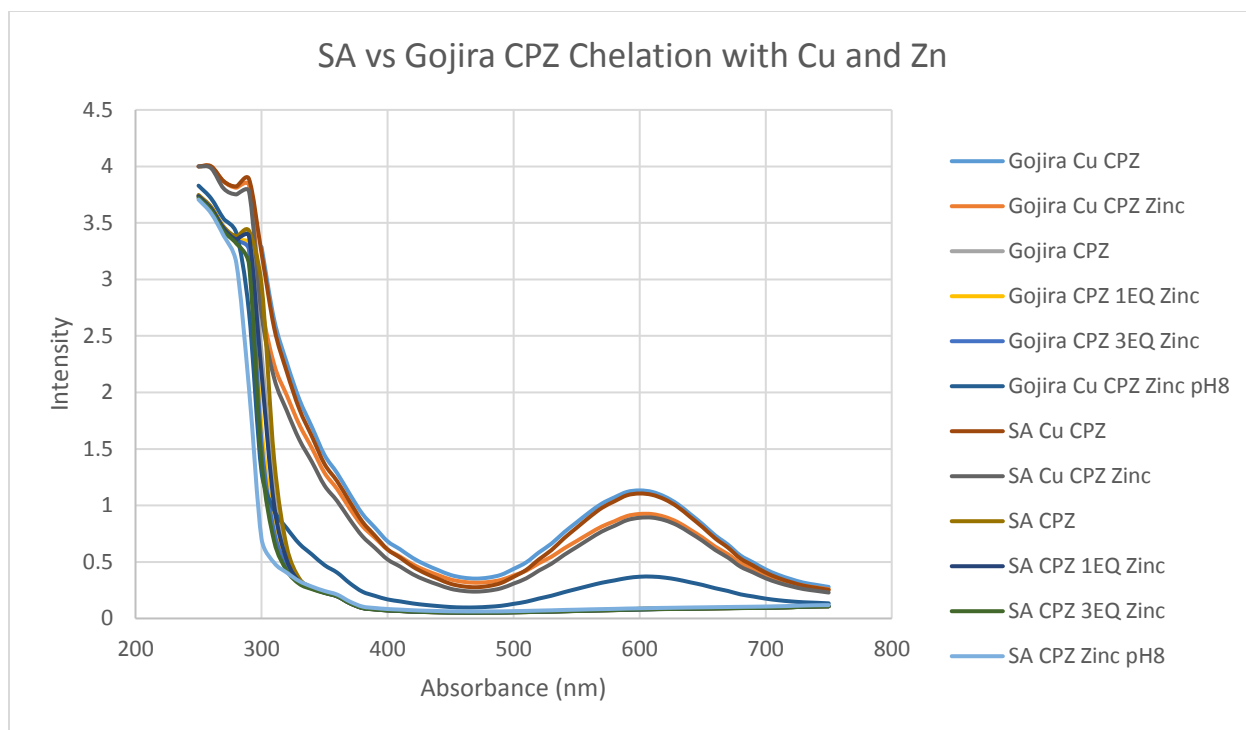


Figure 5. Cumulative graph of both CPZ samples showing absorbance of CPZ solutions with zinc and copper.

It has been proven that CPZ chelates copper, in which the complex has an absorbance around 600 nm. All solutions made with only copper and CPZ had a maximum intensity of 1 at 600 nm, indicating that CPZ chelated copper. All solutions made with zinc and CPZ only had an absorbance reading at 250 nm, suggesting that there was no interaction between the zinc and CPZ (**Figures 5- 7**).

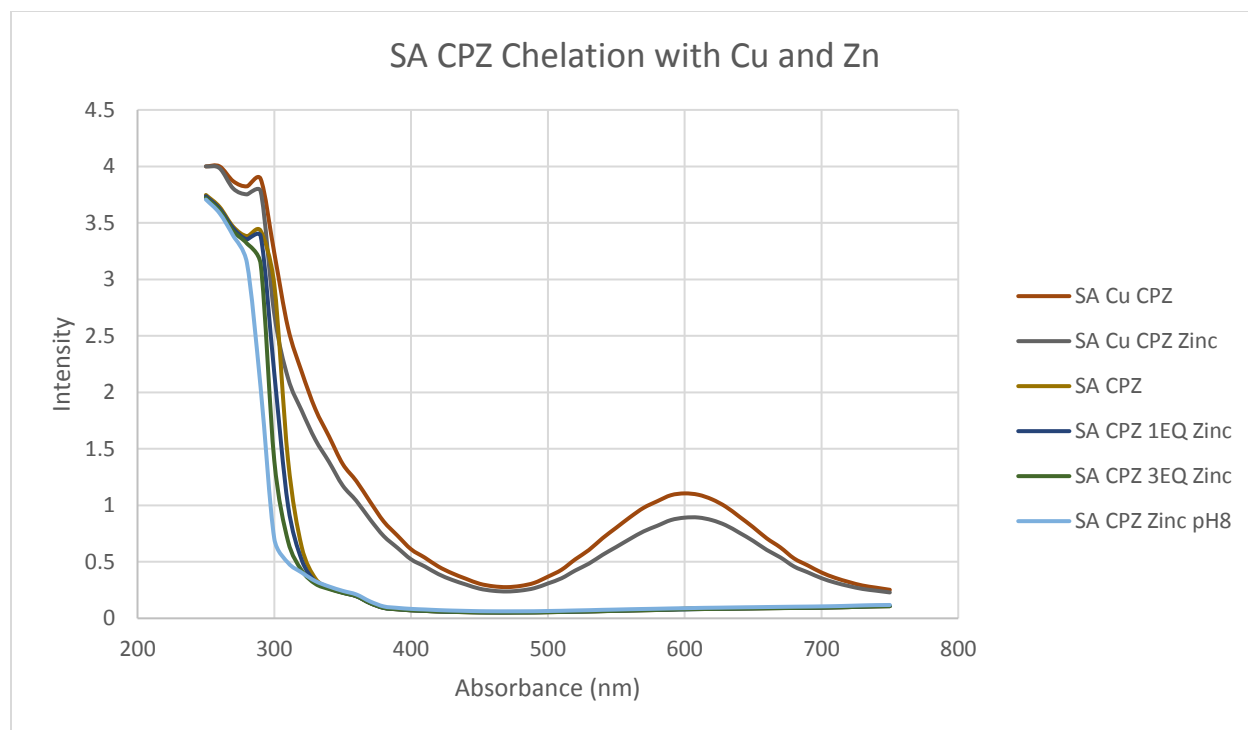


Figure 6. Sigma Aldrich CPZ chelation with zinc and copper.

The solutions with both copper and zinc had a decreased intensity at 600 nm which suggests that there may be interactions between the zinc and copper, the zinc and CPZ, or both that perturbs CPZ from chelating to copper. From this data we confirmed that CPZ readily chelates copper, CPZ does not chelate zinc, and that further analyzation with mass spectrometry can be done to determine the interactions between CPZ, zinc and copper when all added to the same solution.

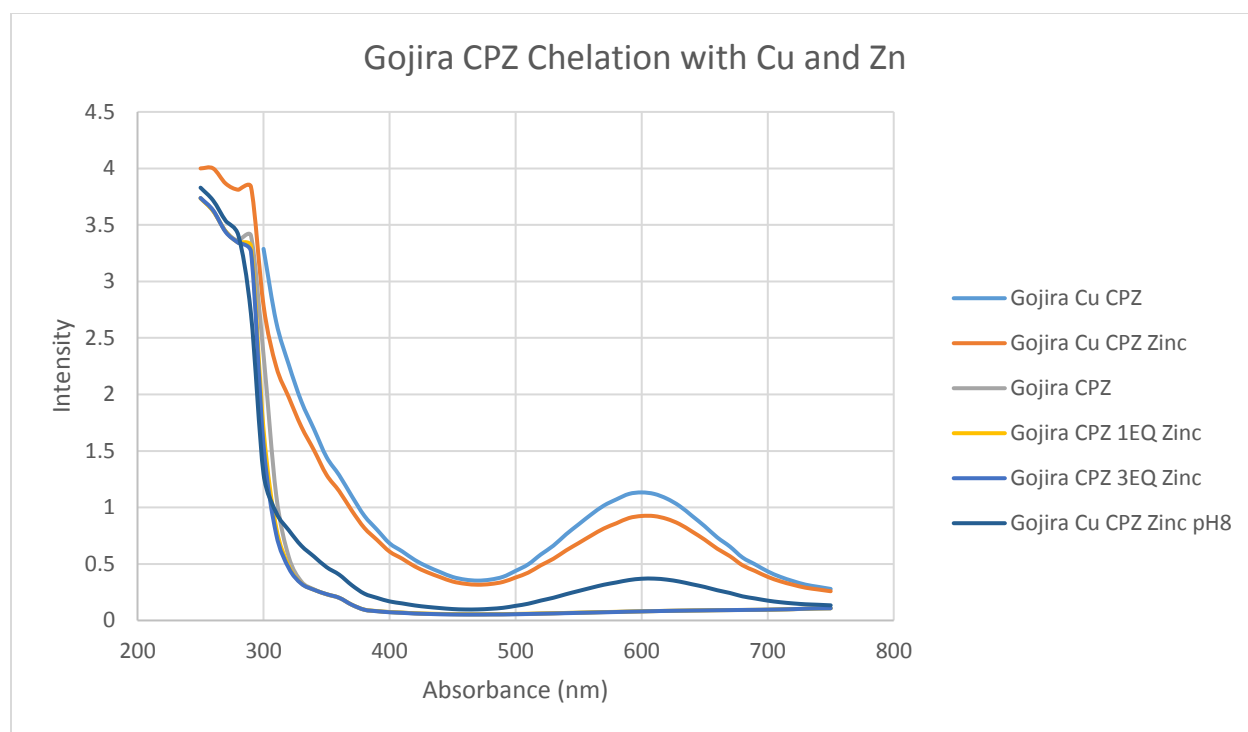


Figure 7. Gojira CPZ chelation with zinc and copper.

CPZ Solubility

There were a total of seven CPZ solutions from the solubility study that went into solution (**Table 4**). Of these solutions, the ones with the lowest concentration (15mM) and highest % EtOH (50%) went into solution the easiest, however this was expected. There were eight solutions that dissolved, but precipitated within 5 minutes after mixing (**Table 4**). The other thirteen solutions did not go into solution (**Table 4**).

Table 4. Results from first CPZ solubility experiment. NS is DMEM no-serum.

IN SOLUTION	FELL OUT < 5 MIN	NOT IN SOLUTION
15 mM 50% EtOH in DMEM	15 mM 30% EtOH in DMEM	15 mM \leq 30% EtOH in HBSS
40 mM 20% EtOH in HBSS	25 mM 50% EtOH in DMEM	25 mM \leq 30% EtOH in DMEM
15 mM 20% EtOH in HBSS	40 mM 20% EtOH in NS	25 mM \leq 50% EtOH in HBSS
15 mM 20% EtOH in NS	15 mM 30% EtOH in NS	40 mM \leq 50% EtOH in DMEM
25 mM 20% EtOH in NS	25 mM 30% EtOH in NS	40 mM \leq 50% EtOH in HBSS
15 mM 50% EtOH in HBSS	25 mM 50% EtOH in NS	40 mM \leq 50% EtOH in NS
15 mM 50% EtOH in NS		

All HBSS solutions had a lot of foam after shaking, and overall, the no serum solutions had the best results. This first solubility experiment showed that CPZ can be dissolved into media. The second solubility experiment took into account the results from the first experiment, and added new steps to improve solubility. The solutions were left to sit longer in the incubator (3 hours), sonication was added, and no-serum media was used since it had the best results in the first solubility experiment. The CPZ went into solution for both Gojira CPZ and Sigma Aldrich CPZ in the second experiment (**Figure 8**).



Figure 8. CPZ solutions that fully dissolved with the two lowest percentages of EtOH (10% and 5%).

This suggests that CPZ needs a lot of time and agitation to fully dissolve into solution, more so than what was done in the first experiment. Heat and sonication are also needed to dissolve CPZ. Finally, using no-serum DMEM mediates the process as well. For following experiments that used CPZ solution, the 10 mM CPZ with 5% EtOH in DMEM no-serum recipe was used since it contained the least amount of EtOH and had the best solubility results.

CPZ Microarray

After receiving the data from the microarray, the lysosomal and mitochondrial pathways were examined for both the 6 hour and 9 hour treatment of CPZ. Overall, there was more dysfunction with the 6 hour treatment than the 9 hour treatment, suggesting that cells are undergoing apoptosis at 9 hours and are shutting off pathways. To verify this, a time study can be done at 1 hour, 2 hours, 6 hours, 9 hours and 12 hours to evaluate CPZ toxicity vs time. Many mitochondrial pathways such as fatty acid oxidation, ETC and mitochondrial fusion were all effected by CPZ at 6 hours of treatment (**Figures 9 and 10**).

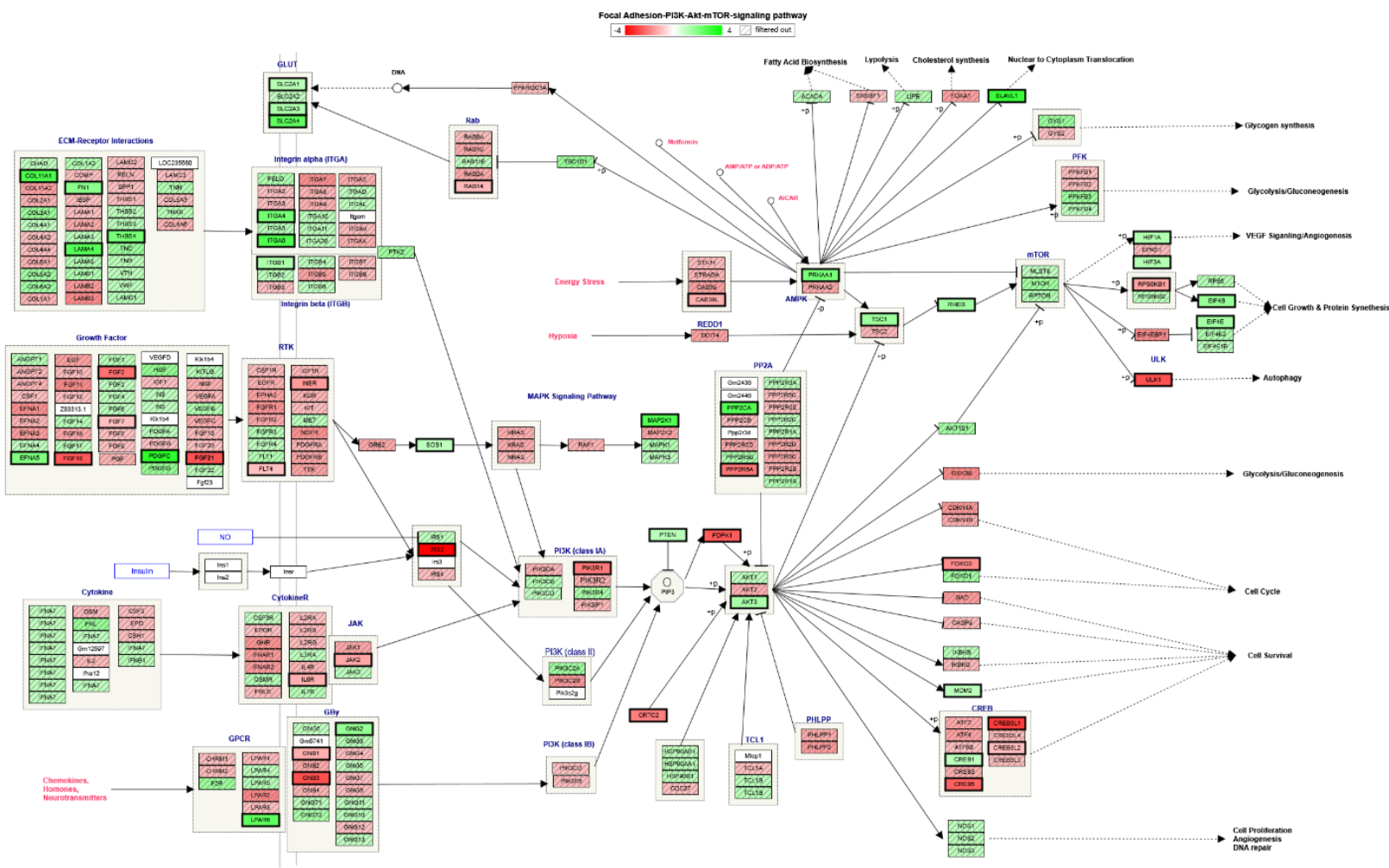


Figure 9. The overall mTOR pathway was affected by CPZ at 6 hours. Image was created by Affymetrix transcriptome analysis software using the CPZ microarray data.

The ETC complex 2 protein succinate dehydrogenase complex subunit D (SDHD), and multiple cytochrome proteins important in transferring electrons were effected by CPZ. This supports the hypothesis that CPZ toxicity acts through mitochondrial ROS and later impacts protein metabolism. Along with mitochondrial dysfunction, lysosomal and mTOR dysfunction were also recorded in the 6 hour CPZ treatment (**Figure 9**).

The diagram illustrates the Electron Transport Chain (OXPHOS system) in mitochondria, showing the flow of electrons (e⁻) and protons (H⁺) through various complexes and proteins. A color scale at the top indicates the electron flow from -4 (red) to 4 (green), with a legend for filtered out components (grey box).

Complex I: NADH-Ubiquinone Oxidoreductase

Complex I is located in the inner mitochondrial membrane. It consists of several subunits, including ND1, ND2, ND3, ND4, ND5, ND6, ND4L, ND4F, ND4F2, ND4F3, ND4F5, ND4F6, ND4F7, ND4F8, ND4F9, ND4F10, ND4F11, ND4F12, ND4F13, ND4F14, ND4F15, ND4F16, ND4F17, ND4F18, ND4F19, ND4F20, ND4F21, ND4F22, ND4F23, ND4F24, ND4F25, ND4F26, ND4F27, ND4F28, ND4F29, ND4F30, ND4F31, ND4F32, ND4F33, ND4F34, ND4F35, ND4F36, ND4F37, ND4F38, ND4F39, ND4F40, ND4F41, ND4F42, ND4F43, ND4F44, ND4F45, ND4F46, ND4F47, ND4F48, ND4F49, ND4F50, ND4F51, ND4F52, ND4F53, ND4F54, ND4F55, ND4F56, ND4F57, ND4F58, ND4F59, ND4F60, ND4F61, ND4F62, ND4F63, ND4F64, ND4F65, ND4F66, ND4F67, ND4F68, ND4F69, ND4F70, ND4F71, ND4F72, ND4F73, ND4F74, ND4F75, ND4F76, ND4F77, ND4F78, ND4F79, ND4F80, ND4F81, ND4F82, ND4F83, ND4F84, ND4F85, ND4F86, ND4F87, ND4F88, ND4F89, ND4F90, ND4F91, ND4F92, ND4F93, ND4F94, ND4F95, ND4F96, ND4F97, ND4F98, ND4F99, ND4F100. The diagram shows the flow of electrons from NADH to ubiquinone (UQ) and then to ubiquinol (UQH₂).

Complex II: Succinate-Ubiquinone Oxidoreductase

Complex II is located in the inner mitochondrial membrane. It consists of several subunits, including SDHA, SDHB, SDHC, SDHD, SDHE, SDHF, SDHG, SDHI, SDHJ, SDHK, SDHL, SDHM, SDHN, SDHO, SDHP, SDHQ, SDHR, SDHS, SDHT, SDHU, SDHV, SDHW, SDHX, SDHY, SDHZ, SDHA1, SDHA2, SDHA3, SDHA4, SDHA5, SDHA6, SDHA7, SDHA8, SDHA9, SDHA10, SDHA11, SDHA12, SDHA13, SDHA14, SDHA15, SDHA16, SDHA17, SDHA18, SDHA19, SDHA20, SDHA21, SDHA22, SDHA23, SDHA24, SDHA25, SDHA26, SDHA27, SDHA28, SDHA29, SDHA30, SDHA31, SDHA32, SDHA33, SDHA34, SDHA35, SDHA36, SDHA37, SDHA38, SDHA39, SDHA40, SDHA41, SDHA42, SDHA43, SDHA44, SDHA45, SDHA46, SDHA47, SDHA48, SDHA49, SDHA50, SDHA51, SDHA52, SDHA53, SDHA54, SDHA55, SDHA56, SDHA57, SDHA58, SDHA59, SDHA60, SDHA61, SDHA62, SDHA63, SDHA64, SDHA65, SDHA66, SDHA67, SDHA68, SDHA69, SDHA70, SDHA71, SDHA72, SDHA73, SDHA74, SDHA75, SDHA76, SDHA77, SDHA78, SDHA79, SDHA80, SDHA81, SDHA82, SDHA83, SDHA84, SDHA85, SDHA86, SDHA87, SDHA88, SDHA89, SDHA90, SDHA91, SDHA92, SDHA93, SDHA94, SDHA95, SDHA96, SDHA97, SDHA98, SDHA99, SDHA100. The diagram shows the flow of electrons from succinate to ubiquinone (UQ) and then to ubiquinol (UQH₂).

Complex III: Ubiquinol-Cytochrome C Reductase

Complex III is located in the inner mitochondrial membrane. It consists of several subunits, including UQCRC1, UQCRC2, UQCRC3, UQCRC4, UQCRC5, UQCRC6, UQCRC7, UQCRC8, UQCRC9, UQCRC10, UQCRC11, UQCRC12, UQCRC13, UQCRC14, UQCRC15, UQCRC16, UQCRC17, UQCRC18, UQCRC19, UQCRC20, UQCRC21, UQCRC22, UQCRC23, UQCRC24, UQCRC25, UQCRC26, UQCRC27, UQCRC28, UQCRC29, UQCRC30, UQCRC31, UQCRC32, UQCRC33, UQCRC34, UQCRC35, UQCRC36, UQCRC37, UQCRC38, UQCRC39, UQCRC40, UQCRC41, UQCRC42, UQCRC43, UQCRC44, UQCRC45, UQCRC46, UQCRC47, UQCRC48, UQCRC49, UQCRC50, UQCRC51, UQCRC52, UQCRC53, UQCRC54, UQCRC55, UQCRC56, UQCRC57, UQCRC58, UQCRC59, UQCRC60, UQCRC61, UQCRC62, UQCRC63, UQCRC64, UQCRC65, UQCRC66, UQCRC67, UQCRC68, UQCRC69, UQCRC70, UQCRC71, UQCRC72, UQCRC73, UQCRC74, UQCRC75, UQCRC76, UQCRC77, UQCRC78, UQCRC79, UQCRC80, UQCRC81, UQCRC82, UQCRC83, UQCRC84, UQCRC85, UQCRC86, UQCRC87, UQCRC88, UQCRC89, UQCRC90, UQCRC91, UQCRC92, UQCRC93, UQCRC94, UQCRC95, UQCRC96, UQCRC97, UQCRC98, UQCRC99, UQCRC100. The diagram shows the flow of electrons from ubiquinol (UQH₂) to cytochrome c (Cyt c) and then to ubiquinone (UQ).

Complex IV: Cytochrome C Oxidase

Complex IV is located in the inner mitochondrial membrane. It consists of several subunits, including COX1, COX2, COX3, COX4, COX5, COX6, COX7, COX8, COX9, COX10, COX11, COX12, COX13, COX14, COX15, COX16, COX17, COX18, COX19, COX20, COX21, COX22, COX23, COX24, COX25, COX26, COX27, COX28, COX29, COX30, COX31, COX32, COX33, COX34, COX35, COX36, COX37, COX38, COX39, COX40, COX41, COX42, COX43, COX44, COX45, COX46, COX47, COX48, COX49, COX50, COX51, COX52, COX53, COX54, COX55, COX56, COX57, COX58, COX59, COX60, COX61, COX62, COX63, COX64, COX65, COX66, COX67, COX68, COX69, COX70, COX71, COX72, COX73, COX74, COX75, COX76, COX77, COX78, COX79, COX80, COX81, COX82, COX83, COX84, COX85, COX86, COX87, COX88, COX89, COX90, COX91, COX92, COX93, COX94, COX95, COX96, COX97, COX98, COX99, COX100. The diagram shows the flow of electrons from cytochrome c (Cyt c) to oxygen (O₂) and then to water (H₂O).

Complex V: ATP Synthase F1 Complex

Complex V is located in the inner mitochondrial membrane. It consists of several subunits, including ATP5A1, ATP5B1, ATP5C1, ATP5D1, ATP5E1, ATP5F1, ATP5G1, ATP5H1, ATP5I1, ATP5J1, ATP5K1, ATP5L1, ATP5M1, ATP5N1, ATP5O1, ATP5P1, ATP5Q1, ATP5R1, ATP5S1, ATP5T1, ATP5U1, ATP5V1, ATP5W1, ATP5X1, ATP5Y1, ATP5Z1, ATP5A2, ATP5A3, ATP5A4, ATP5A5, ATP5A6, ATP5A7, ATP5A8, ATP5A9, ATP5A10, ATP5A11, ATP5A12, ATP5A13, ATP5A14, ATP5A15, ATP5A16, ATP5A17, ATP5A18, ATP5A19, ATP5A20, ATP5A21, ATP5A22, ATP5A23, ATP5A24, ATP5A25, ATP5A26, ATP5A27, ATP5A28, ATP5A29, ATP5A30, ATP5A31, ATP5A32, ATP5A33, ATP5A34, ATP5A35, ATP5A36, ATP5A37, ATP5A38, ATP5A39, ATP5A40, ATP5A41, ATP5A42, ATP5A43, ATP5A44, ATP5A45, ATP5A46, ATP5A47, ATP5A48, ATP5A49, ATP5A50, ATP5A51, ATP5A52, ATP5A53, ATP5A54, ATP5A55, ATP5A56, ATP5A57, ATP5A58, ATP5A59, ATP5A60, ATP5A61, ATP5A62, ATP5A63, ATP5A64, ATP5A65, ATP5A66, ATP5A67, ATP5A68, ATP5A69, ATP5A70, ATP5A71, ATP5A72, ATP5A73, ATP5A74, ATP5A75, ATP5A76, ATP5A77, ATP5A78, ATP5A79, ATP5A80, ATP5A81, ATP5A82, ATP5A83, ATP5A84, ATP5A85, ATP5A86, ATP5A87, ATP5A88, ATP5A89, ATP5A90, ATP5A91, ATP5A92, ATP5A93, ATP5A94, ATP5A95, ATP5A96, ATP5A97, ATP5A98, ATP5A99, ATP5A100. The diagram shows the flow of protons (H⁺) from the intermembrane space to the matrix, driving the synthesis of ATP from ADP and inorganic phosphate (P_i).

Uncoupling Protein

Uncoupling Protein (UCP) is located in the inner mitochondrial membrane. It consists of several subunits, including UCP1, UCP2, UCP3, UCP4, UCP5, UCP6, UCP7, UCP8, UCP9, UCP10, UCP11, UCP12, UCP13, UCP14, UCP15, UCP16, UCP17, UCP18, UCP19, UCP20, UCP21, UCP22, UCP23, UCP24, UCP25, UCP26, UCP27, UCP28, UCP29, UCP30, UCP31, UCP32, UCP33, UCP34, UCP35, UCP36, UCP37, UCP38, UCP39, UCP40, UCP41, UCP42, UCP43, UCP44, UCP45, UCP46, UCP47, UCP48, UCP49, UCP50, UCP51, UCP52, UCP53, UCP54, UCP55, UCP56, UCP57, UCP58, UCP59, UCP60, UCP61, UCP62, UCP63, UCP64, UCP65, UCP66, UCP67, UCP68, UCP69, UCP70, UCP71, UCP72, UCP73, UCP74, UCP75, UCP76, UCP77, UCP78, UCP79, UCP80, UCP81, UCP82, UCP83, UCP84, UCP85, UCP86, UCP87, UCP88, UCP89, UCP90, UCP91, UCP92, UCP93, UCP94, UCP95, UCP96, UCP97, UCP98, UCP99, UCP100

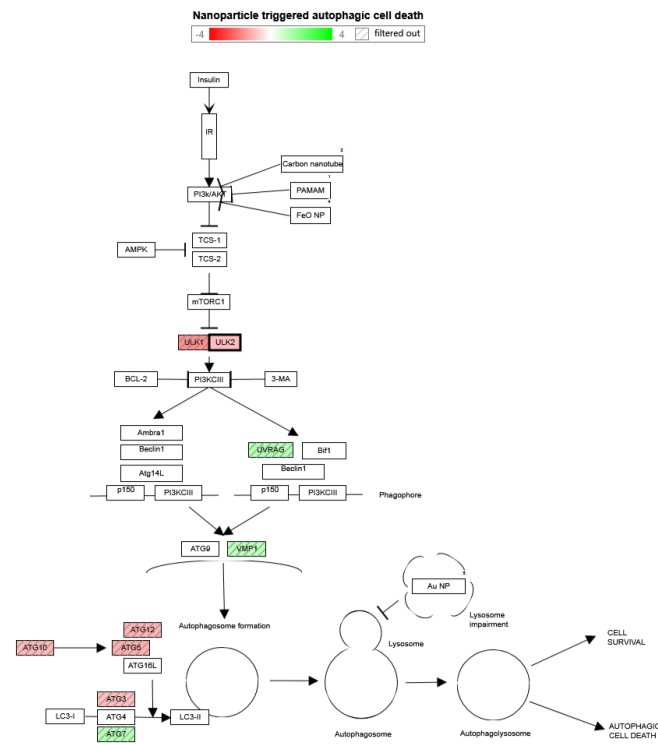


Figure 11. Disruptions in autophagy pathway after 9 hours of CPZ toxicity. Image was created by Affymetrix transcriptome analysis software using the CPZ microarray data.

There was also significant dysregulation in mTOR related pathways, one of these genes coding for the protein Growth Factor Receptor Protein 10 (GRB10) which is involved with signal transduction via receptor tyrosine kinase pathways (**Figure 12**).¹⁷ Other proteins affected in the mTOR pathway after 9 hours of CPZ treatment included EIF4G1 involved in protein translation and LAMTOR3, a late endosomal and lysosomal adaptor protein (**Figure 12**).^{18,19}

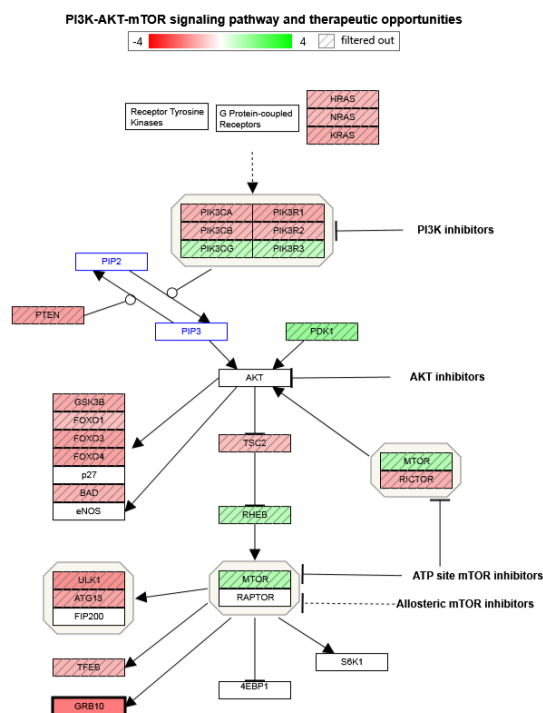


Figure 12. CPZ disruption of mTOR pathway after 9 hours. Image was created by Affymetrix transcriptome analysis software using the CPZ microarray data.

All of these genes code for proteins related to signal transduction, suggesting that CPZ disrupts normal cellular function and induces autophagy. Overall, from this data, we suggest that CPZ causes mitochondrial and lysosomal dysfunction, and that the disruption of these pathways are linked through CPZ interference with mTOR signaling.

Leucine Supplementation MTT Assay

Many MTT assays were conducted for this experiment with mixed results. Most of the assays resulted in the vehicle, CPZ, or both killing the cells. Leucine supplementation did not significantly reverse CPZ toxicity in the assays that were done. From the results gathered, the data suggests that addition 0.2 mM leucine was most successful in rescuing cells from CPZ (**Figure 13**). The cells treated with CPZ only had around 55% viability. The vehicle was 3%

EtOH which had a viability of around 85% compared to the untreated cells (**Figure 13**). This suggests that the EtOH added along with the CPZ does not effectively kill cells for this given assay. As treatment concentration of leucine increased past 0.2 mM to 0.4 mM, 0.6 mM and 0.8 mM, the viability had no significant change after a drop from 60% viability at 0.2 mM to 45% viability for the latter treatments (**Figure 13**).

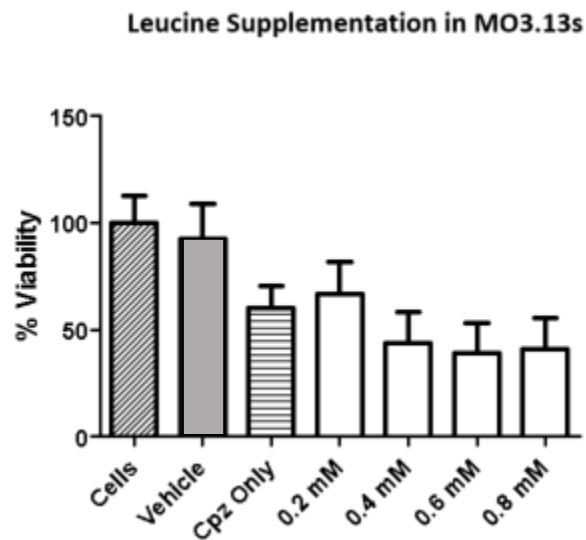


Figure 13. Cell viability after cell rescue experiment with varying concentrations of leucine added to CPZ affected cells. Vehicle represents EtOH without CPZ. Cells represents no addition of treatment.

The error bars on this graph are large, which means that the data may not be significant, however this assay provided good suggestions as to where to take this project in future experiments. Allowing for CPZ to effect cells for longer than 24 hours may decrease variation in results. Also treating with leucine at different concentrations such as 0.05 mM, 0.1mM, 1 mM, 1.5 mM and 2 mM would help focus the most effective treatment concentration for leucine. As mentioned previously, after running the assays, it was discovered that CPZ could be dissolved in EtOH at 1% final EtOH treatment concentration which would also assure that the vehicle is not

killing the cells. Overall, leucine supplementation is likely to affect CPZ toxicity however further experiments will have to be conducted to confirm this hypothesis.

CPZ Induced Lysosomal Imaging:

To determine morphology of lysosomes during CPZ toxicity, C₁₀ and C₁₁ lysosomal probes provided by Dr. Pang's lab were used to target lysosomes via fluorescent imaging. Both probes were verified to target lysosomes, however it was observed that the probes may have targeted nuclear proteins as well. Originally, the C₁₀ probe was not yet verified to work in fixed imaging. This experiment proved that the C₁₀ probe was successful in targeting lysosomes following a fixed imaging protocol. The C₁₁ probe was already verified to work, and it did in this experiment. Along with the lysosomal probes, DAPI was used to stain the nuclei to verify location and overall health of the cell. The cells treated with only EtOH for both C₁₀ and C₁₁ probes exhibited more distribution of lysosomes throughout the cell (**Figures 14 and 15**).

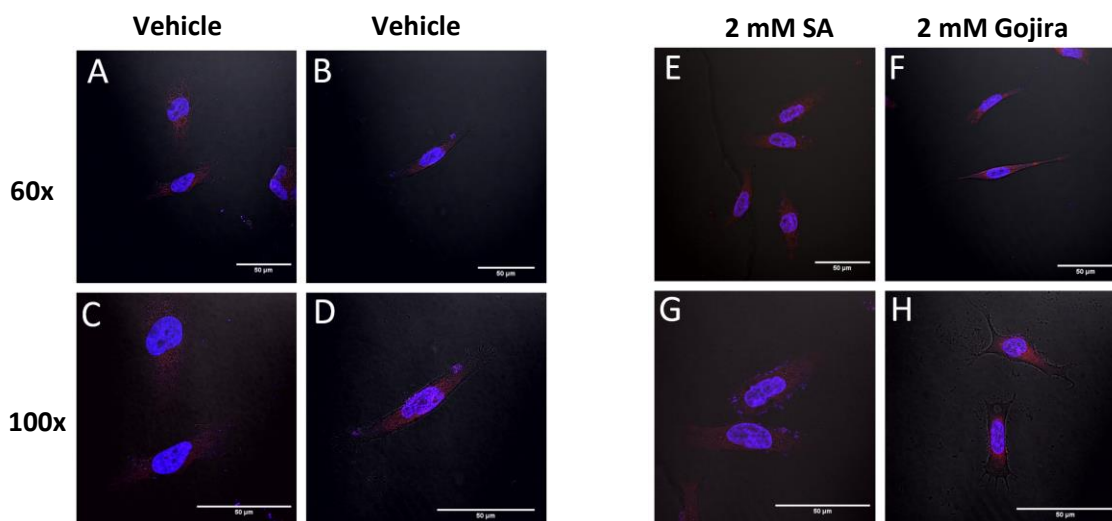


Figure 14. MO3.13 cells stained with C₁₀ (A and C) and C₁₁ red lysosomal probe (B, D, E, F, G and H). All samples were stained with blue DAPI to show nuclei. A, B, C and D are 1% EtOH vehicle at 60x (A and B) and 100x (C and D). E and G are 2 mM SA CPZ at 60x (A) and 100x (C). F and H are 2 mM Gojira CPZ at 60x (B) and 100x (D). Scale bar for all image is set to 50 μ m.

The treatment of SA CPZ vs Gojira CPZ made no significance difference in the lysosomal morphology of the cells. The cells treated with CPZ exhibited more intense fluorescence of lysosomes around the nucleus compared to the EtOH treated cells without CPZ (**Figure 14**). This suggests that lysosome production is upregulated under CPZ toxicity to account for increased autophagy related signals.

The 2 mM SA CPZ was imaged with both C₁₀ and C₁₁ lysosomal probes (**Figure 15**). Similar to the EtOH treatment, it was observed that the C₁₀ probe, originally not proven to work in fixed cells, appears slightly sharper than the C₁₁ probe. The difference isn't drastic, but it is noticeable (**Figures 14 and 15**). The cells that were not treated with EtOH or CPZ had similar morphology to the treatment cells, however similar to the EtOH treated cells, the lysosomes appear to have a wider distribution (**Figure 15**).

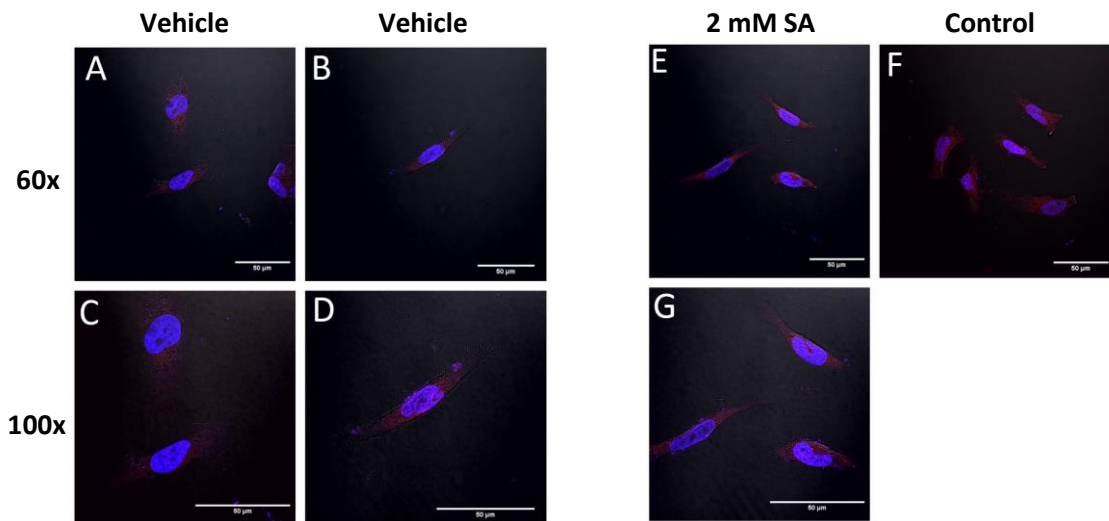


Figure 15. . MO3.13 cells stained with C₁₀ (A, C, E and G) and C₁₁ red lysosomal probe (B, D and F). All samples were stained with blue DAPI to show nuclei. A, B, C and D are 1% EtOH vehicle at 60x (A and B) and 100x (C and D). E and G are 2 mM SA CPZ at 60x (E) and 100x (G). F is MO3.13 cells with no treatment at 60x. Scale bar for all image is set to 50 μm.

This experiment provided an insight on the morphology and pathology of lysosomes during CPZ toxicity. Although differences between the treatment groups and control groups were

miniscule, there were slight differences seen in the distribution and localization of the lysosomes; The CPZ treated cells had a higher concentration of lysosomes localized around the nucleus than that of the vehicle and control. The microarray data supports that lysosomal and mitochondrial function is disrupted by CPZ toxicity. The images of the 2 mM CPZ treatments show slight increases in intensity of the lysosomal probe signal, as well as more concentration localization around the nucleus. Taken from this, it is possible that the introduction of CPZ upregulates lysosomal production by disrupting lysosomal and mitochondrial function, thus increasing autophagy related pathways.

Conclusion

The neurotoxic effects of cuprizone allow it to be used as a common model of demyelination and simulator of neurodegenerative disease both *in vivo* and *in vitro*.^{6,20} The human MO3.13 oligodendrocyte cell line exhibits alterations to normal metabolism among introduction to CPZ.²⁰ Through this model, further effects of CPZ on neurotoxicity were examined in this experiment using MO3.13s as a model. CPZ is most known for its ability to chelate copper, however it was previously unclear whether or not CPZ could chelate the neighbor of copper on the periodic table, zinc. The results from the CPZ chelation experiment suggest that CPZ does not chelate zinc as efficiently as it does copper, however zinc may perturb the efficiency of copper-CPZ chelation (**Figures 5-7**). This experiment also discovered advances in CPZ solubility with a decreased percentage of EtOH needed for CPZ to fully dissolve (**Figure 8**). With this, the vehicle in cell experiments will be much less likely to cause variation in the treatment. The microarray data obtained from CPZ treatment of 6 hours and 9 hours show extreme disruption in major lysosomal and mitochondrial pathways, including mTOR, ETC, and autophagy (**Figures 9-12**). Cumulatively, this data demonstrates the crosstalk between lysosomal

and mitochondrial regulation, and how CPZ can perturb normal signaling. The supplementation of leucine to rescue cells from CPZ toxicity was also tested in this experiment (**Figure 13**).

Overall, the results of the viability assays were not conducive, however they provide direction for further experiments. The lowest treatment concentration, 0.2 mM of leucine had the highest cell viability, higher than CPZ treatment alone (**Figure 13**). To further test leucine initiated cell rescue from CPZ, a wider range of leucine treatment concentrations can be tested to narrow the ideal treatment concentration for rescue. Lysosomal imaging using C₁₀ and C₁₁ probes provided information on localization and morphology of lysosomes when subjected to CPZ (**Figures 14 and 15**). Although differences were slight, overall, CPZ treated cells exhibited increased lysosome localization around the nucleus and increased intensity. This data suggests that CPZ may upregulate lysosome production. For all experiments, both Sigma Aldrich and Gojira brand CPZ were used. There were no observable differences between the two brands of CPZ. Taken altogether, this experiment has provided new advancements in CPZ solubility and has provided evidence that introduction of CPZ can cause lysosomal and mitochondrial dysfunction which ultimately leads to increased cell death through autophagy.

Acknowledgments

I would like to sincerely thank my graduate students Celina Cahalane, Gardenia Pacheco, Hannah Baumann, Kayla Adkins-Travis, Nino Kovaljesko, Jillian Kodger and Alexandra Taraboletti for all of their patience, assistance and mentorship they have given me during this process. I would also like to sincerely thank Dr. Shriver for her extensive knowledge, guidance and supervision as she allowed me to partake in her research. Funding for this project was provided by the University of Akron and the 1R15 GM119074-01 (L.P.S.) grant.

References

- (1) Bunge, R. P. *Glial Cells and the Central Myelin Sheath*; 1968.
- (2) Merrill, J. E.; Scolding, N. J. Mechanisms of Damage to Myelin and Oligodendrocytes and Their Relevance to Disease. *Neuropathol. Appl. Neurobiol.* **1999**, 25 (6), 435–458.
- (3) Buntinx, M.; Vanderlocht, J.; Hellings, N.; Vandenabeele, F.; Lambrichts, I.; Raus, J.; Ameloot, M.; Stinissen, P.; Steels, P. Characterization of Three Human Oligodendroglial Cell Lines as a Model to Study Oligodendrocyte Injury: Morphology and Oligodendrocyte-Specific Gene Expression. *J. Neurocytol.* **2003**, 32 (1), 25–38.
- (4) Boscia, F.; D’Avanzo, C.; Pannaccione, A.; Secondo, A.; Casamassa, A.; Formisano, L.; Guida, N.; Annunziato, L. Silencing or Knocking out the Na⁺/Ca²⁺ Exchanger-3 (NCX3) Impairs Oligodendrocyte Differentiation. *Cell Death Differ.* **2012**, 19 (4), 562–572.
- (5) Matsushima, G. K.; Morell, P. The Neurotoxicant, Cuprizone, as a Model to Study Demyelination and Remyelination in the Central Nervous System. *Brain Pathol.* **2006**, 11 (1), 107–116.
- (6) Praet, J.; Guglielmetti, C.; Berneman, Z.; Van der Linden, A.; Ponsaerts, P. Cellular and Molecular Neuropathology of the Cuprizone Mouse Model: Clinical Relevance for Multiple Sclerosis. *Neurosci. Biobehav. Rev.* **2014**, 47, 485–505.
- (7) Lambdin, C. E.; Taylor, W. V. Determination of Trace Copper in Petroleum Middle Distillates with Cuprizone. *Anal. Chem.* **1968**, 40 (14), 2196–2197.
- (8) Zatta, P.; Raso, M.; Zambenedetti, P.; Wittkowski, W.; Messori, L.; Piccioli, F.; Mauri, P. L.; Beltramini, M. Copper and Zinc Dismetabolism in the Mouse Brain upon Chronic Cuprizone Treatment. *Cell. Mol. Life Sci.* **2005**, 62 (13), 1502–1513.
- (9) Horn, D.; Barrientos, A. Mitochondrial Copper Metabolism and Delivery to Cytochrome c Oxidase. *IUBMB Life* **2008**, 60 (7), 421.
- (10) Horng, Y.-C.; Cobine, P. A.; Maxfield, A. B.; Carr, H. S.; Winge, D. R. Specific Copper Transfer from the Cox17 Metallochaperone to Both Sco1 and Cox11 in the Assembly of Yeast Cytochrome C Oxidase. *J. Biol. Chem.* **2004**, 279 (34), 35334–35340.
- (11) Faizi, M.; Salimi, A.; Seydi, E.; Naserzadeh, P.; Kouhnavard, M.; Rahimi, A.; Pourahmad, J. Toxicity of Cuprizone a Cu²⁺ Chelating Agent on Isolated Mouse Brain Mitochondria: A Justification for Demyelination and Subsequent Behavioral Dysfunction. *Toxicol. Mech. Methods* **2016**, 26 (4), 276–283.
- (12) Taraboletti, A.; Walker, T.; Avila, R.; Huang, H.; Caporoso, J.; Manandhar, E.; Leeper, T. C.; Modarelli, D. A.; Medicetty, S.; Shriver, L. P. Cuprizone Intoxication Induces Cell Intrinsic Alterations in Oligodendrocyte Metabolism Independent of Copper Chelation. *Biochemistry* **2017**, 56 (10), 1518–1528.
- (13) Harris, R. A.; Joshi, M.; Jeoung, N. H.; Obayashi, M. Overview of the Molecular and Biochemical Basis of Branched-Chain Amino Acid Catabolism. *J. Nutr.* **2005**, 135 (6), 1527S–1530S.

- (14) Alers, S.; Löffler, A. S.; Wesselborg, S.; Stork, B. Role of AMPK-MTOR-Ulk1/2 in the Regulation of Autophagy: Cross Talk, Shortcuts, and Feedbacks. *Mol. Cell. Biol.* **2012**, *32* (1), 2–11.
- (15) Yu, L.; McPhee, C. K.; Zheng, L.; Mardones, G. A.; Rong, Y.; Peng, J.; Mi, N.; Zhao, Y.; Liu, Z.; Wan, F.; et al. Termination of Autophagy and Reformation of Lysosomes Regulated by MTOR. *Nature* **2010**, *465* (7300), 942–946.
- (16) Stone, S.; Lin, W. The Unfolded Protein Response in Multiple Sclerosis. *Front. Neurosci.* **2015**, *9*, 264.
- (17) Sokolova, G. P. [The Fatty Acid Composition of the Brain and Their Biosynthesis (Review of the Current Literature)]. *Nervn. Sist.* **1975**, *15*, 35–59.
- (18) Mitsui, Y. [Corneal Infections (Author's Transl)]. *Nihon. Ganka Gakkai Zasshi* **1975**, *79* (11), 1651–1664.
- (19) Beex, L. V.; Ross, A.; Smals, A. G.; Kloppenborg, P. W. Letter: 5-Fluorouracil and the Thyroid. *Lancet (London, England)* **1976**, *1* (7964), 866–867.
- (20) Taraboletti, A.; Walker, T.; Avila, R.; Huang, H.; Caporoso, J.; Manandhar, E.; Leeper, T. C.; Modarelli, D. A.; Medicetty, S.; Shriver, L. P. Cuprizone Intoxication Induces Cell Intrinsic Alterations in Oligodendrocyte Metabolism Independent of Copper Chelation. *Biochemistry* **2017**, *56* (10), 1518–1528.

Appendix 1

Safety Considerations

All experiments in this lab were conducted in a ventilated hood with gloves following safety protocol. All reagents were sterilized with 70% EtOH before entering the hood and after leaving the hood. The hood was sprayed with 70% EtOH before and after use. After every experiment in the hood, the UV light was turned on for 10 minutes to sterilize. All waste from cell culture experiments were neutralized with 50% bleach before discarding in biohazard waste. To reduce the risk of contamination, the water bath, incubator and sonicator were routinely cleaned with 70% EtOH every week and replaced with autoclaved water if necessary. Some reagents that were used in this lab are toxic substances. Goggles and a face mask were used when weighing harmful chemicals such as paraformaldehyde. Cuprizone is a toxic chemical that can be harmful if ingested. This chemical was handled with gloves in a well ventilated area. Paraformaldehyde is a preservative that is toxic to humans. Paraformaldehyde was handled under a hood. Sodium Hydroxide and Hydrochloric acid were used to adjust the pH of solutions. These chemicals can cause burns if exposed to skin. Gloves were used when dealing with these solutions in the hood. The protease, Trypsin, was used to cleave cells from the culture plates. Trypsin is a lysing agent. It was strictly used in the hood with gloves on. All utensils that were used in cell experiments were autoclaved after use. Before and after lab work, hands were washed to decrease contamination. The lab that the research was conducted in is equipped with a safety shower, a fire extinguisher and a first aid kit. All of these safety devices were made accessible during experiments.